Analyst

Accepted Manuscript

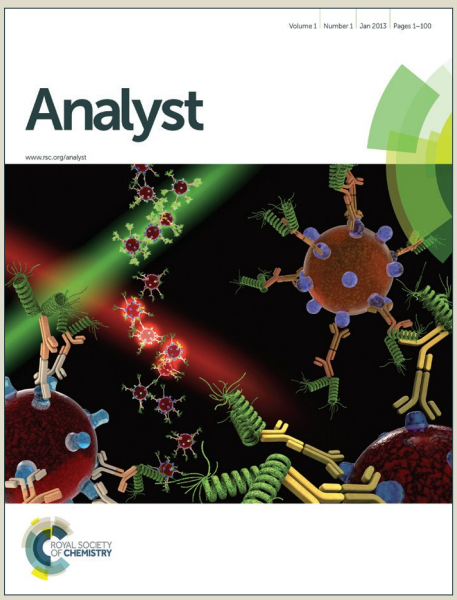

ROYAL SOCIETY OF CHEMISTRY

www.rsc.org/analyst

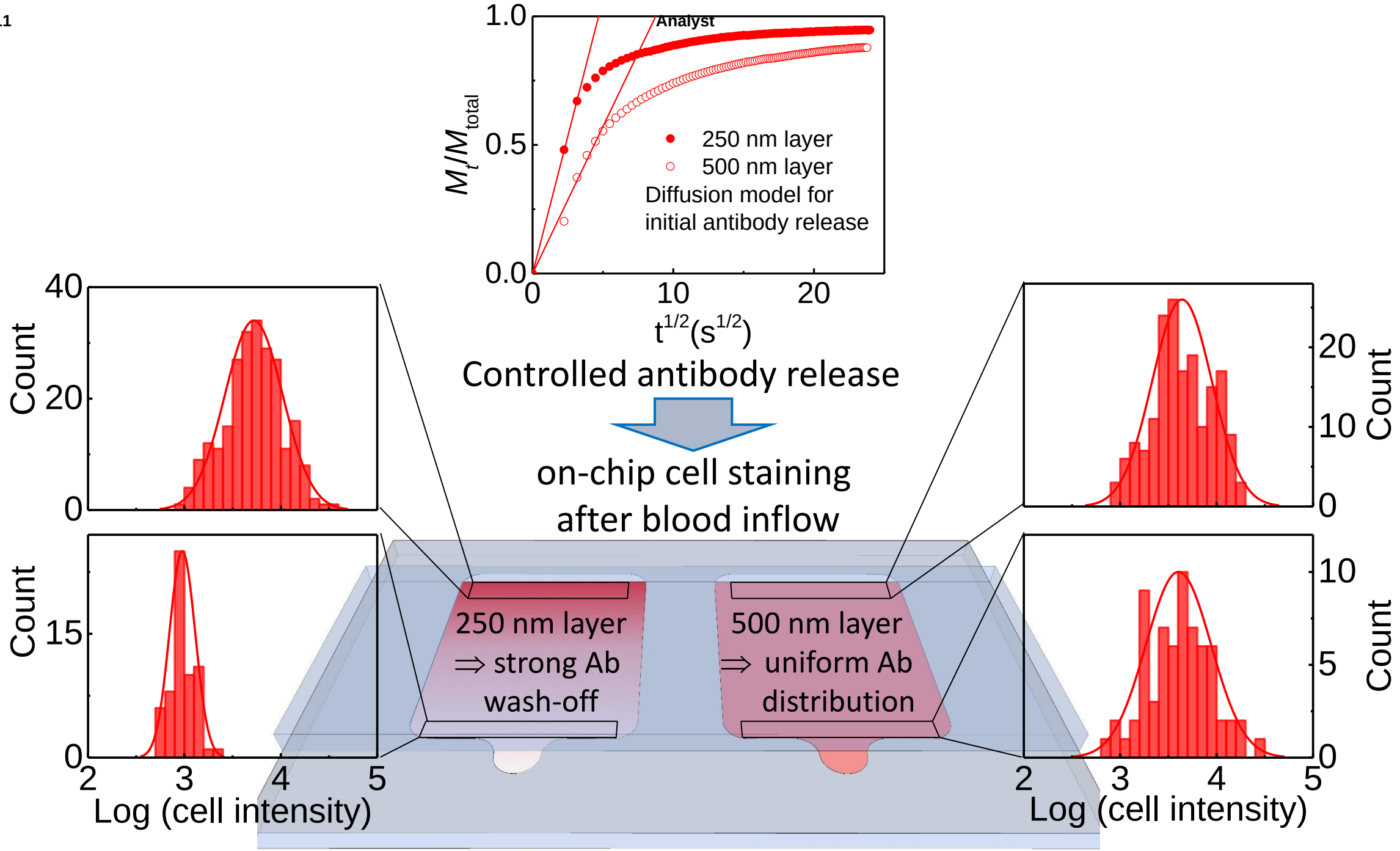

Gelatin layers tailored for controlled release of antibody allow for optimized on-chip immunostaining of leukocytes in whole blood.

Journal Name

ARTICLE

Controlled antibody release from gelatin for on-chip sample preparation

Received 00th January 20xx,
Accepted 00th January 20xx

DOI: 10.1039/x0xx00000x

www.rsc.org/

Xichen Zhang[a], Dorothee Wasserberg[a], Christian Breukers[a], Leon W.M.M. Terstappen[a] and Markus Beck*[a]

A practical way to realize on-chip sample preparation for point-of-care diagnostics is to store the required reagents on a microfluidic device and release them in a controlled manner upon contact with the sample. For the development of such diagnostic devices, a fundamental understanding of the release kinetics of reagents from suitable materials in microfluidic chips is therefore essential. Here, we study the release kinetics of fluorophore-conjugated antibodies from (sub-) µm thick gelatin layers and several ways to control the release time. The observed antibody release is well-described by a diffusion model. Release times ranging from ~20 s to ~650 s were determined for layers with thicknesses (in the dry state) between 0.25 µm and 1.5 µm, corresponding to a diffusivity of 0.65 µm^2/s (in the swollen state) for our standard layer preparation conditions. By modifying the preparation conditions, we can influence the properties of gelatin to realize faster or slower release. Faster drying at increased temperatures leads to shorter release times, whereas slower drying at increased humidity yields slower release. As expected in a diffusive process, the release time increases with the size of the antibody. Moreover, the ionic strength of the release medium has a significant impact on the release kinetics. Applying these findings to cell counting chambers with on-chip sample preparation, we can tune the release to control the antibody distribution after inflow of blood in order to achieve homogeneous cell staining.

Introduction

One of the major fields of applications for microfluidics is *in vitro* diagnostics, with great potential particularly in point-of-care diagnostics.[1-3] Many process steps and sensing principles have been realized on microfluidic devices.[4] Recently, on-chip sample preparation using reagents stored in microfluidic devices has received more and more attention.[5] On-chip sample preparation can eliminate the dependence on external instrumentation for reagent delivery as well as benchtop sample treatment, thus integrating the complete test into one disposable.[6] To realize on-chip sample preparation, reagents are integrated in microfluidic devices and released upon contact with the inflowing sample. Compared with liquid reagents[7-10], integrating dry reagents in microfluidic devices is beneficial for long-term storage and convenient for transportation, due to the better stability of reagents in the dry state.[11] However, the controlled dissolution of the reagent and on-chip mixing with the added sample is challenging. Especially in applications where the inflowing sample passes a reservoir of the reagent and slowly dissolves or washes out the stored reagent[12-15], very precise control of the sample flow and the reagent release process is required. In contrast, mixing between sample and reagents in stopped flow applications can be realized simply by releasing the reagent with sufficient delay after the sample inflow has stopped at the required position on the chip.[16] To realize controlled reagent release, hydrogels with embedded reagents in microfluidics chambers have been employed in the past. It has been shown that sample inflow can induce swelling due to rehydration[17] or a change in pH[18] and lead to subsequent diffusion of reagents out of the hydrogel matrix.

We previously demonstrated this principle for on-chip sample preparation in cell counting chambers for the enumeration of CD4-positive (CD4$^+$) T-lymphocytes in a stopped-flow configuration.[17] In short, our cell counting chambers contain a dry gelatin layer with embedded fluorescently labeled antibody for the immunostaining of T-lymphocytes. Inflowing blood initiates the rehydration (i.e. swelling) of the gelatin matrix but release only starts after a certain level of rehydration has been reached. The layers are tailored in such a way, that the inflow of blood takes place, while rehydration is not yet sufficient for antibody release. However, after the chamber is filled and the flow has stopped, rehydration rapidly reaches levels that enable release. The

[a] *Medical Cell Biophysics, MIRA Institute for Biomedical Technology and Technical Medicine, Faculty of Science and Technology, PO Box 217, 7500 AE Enschede, The Netherlands. E-mail: M.Beck@utwente.nl*

† Blood donors were healthy individuals at the University of Twente that provided written informed consent. All experiments were performed in compliance with the relevant laws and institutional guidelines.

Electronic Supplementary Information (ESI) available: Supplementary information shows the reproducibility of device fabrication (ESI S1), the influence of flow rates on release kinetics (ESI S2), the statistical analysis of different release kinetics (ESI S3), the calibration of antibody embedded in the gelatin layers (ESI S4) and FT-IR spectra of differently prepared gelatin layers (ESI S5, Table S1). See DOI: 10.1039/x0xx00000x

delayed release after inflow (into a static sample) ensures, that wash-off of antibody during inflow is largely prevented, and that the released antibody is distributed homogeneously throughout the chamber. Homogeneous antibody release is a prerequisite for uniform cell staining, which is of paramount importance to our cell counting application: In our imaging setup we chose a wide field of view at low magnification in order to image a large volume at once, and can therefore identify stained cells only via their fluorescence intensity. If the staining is inhomogeneous the definition of selection criteria like an intensity threshold becomes problematic.

To further optimize the delayed release, a fundamental understanding of the release kinetics is essential. Conventional release studies generally focus on long-term release within hours or days from polymer layers tens of µm to mm thick for the purpose of *in vivo* drug delivery.[19] Microfluidics applications generally require thinner layers and shorter release times. Our cell counting application, for instance, requires sub-µm gelatin layers to release fluorescently labeled antibody on timescales between 10 seconds and a few minutes. This range is pre-determined by the time needed to fill the chamber by capillary action (between 2 s and 10 s, representing the lower limit for the release) and the incubation time for immunostaining (typically 5 min to 30 min, during which sufficient antibody has to be released).

Here, we report methods to monitor and influence the release of antibodies from gelatin in flow chambers. In our release experiments, a medium was passed through a flow chamber coated on one side with a dry gelatin layer containing fluorescently labeled antibody, and the decrease of fluorescence intensity during release was monitored over time. The measured release kinetics was found to be consistent with a diffusion-controlled release model. Various parameters including layer thickness, drying conditions (temperature and humidity), antibody size and the ionic strength of the medium allowed us to tune the release kinetics. Moreover, we verified that the release kinetics determine the antibody distribution as well as the homogeneity of cell staining in a counting chamber after sample inflow.

Experiments

Flow chamber and cell counting chamber fabrication

The assembled flow chamber is shown schematically in Fig. 1a and 1b. Precut laminating adhesive (nominal thickness 25.4 µm, 3M) was attached to a poly(methyl methacrylate) (PMMA) substrate to create the flow channel (4.8 mm × 61 mm). The subsequent attachment of poly(tetrafluoroethylene) (PTFE) tape determined the casting area (4.8 mm × 4 mm) for the gelatin (type A, bloom 295, Sigma)/antibody-conjugate solution. The solution was left to dry to form a layer of typically a few hundred nm thickness. The PTFE tape was removed prior to the attachment of a capping glass slide (standard microscope slide, Menzel) with two holes for tubing connection. Actual chamber heights around 27 µm were determined interferometrically. Details on the reproducibility of device

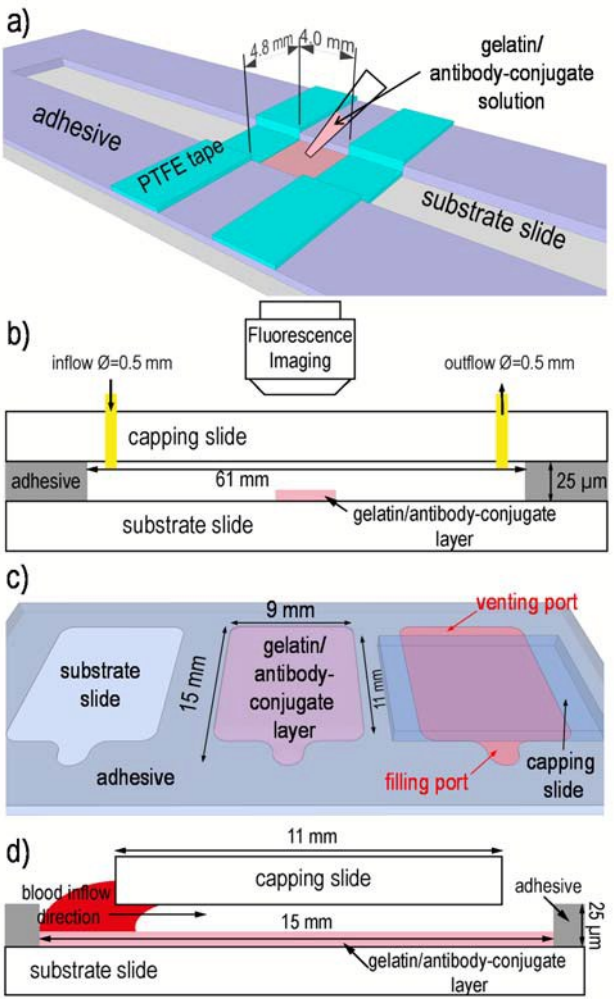

Fig. 1: Schematic representations of flow chambers (a) perspective view, (b) side view and cell counting chambers (c) perspective view, (d) side view.

fabrication can be found in the ESI section "Reproducibility of the gelatin layers prepared using 'standard conditions' and chamber heights". The fabrication of cell counting chambers (Fig. 1c and 1d) is described in detail elsewhere.[17] Briefly, the gelatin/antibody-conjugate layer was cast in a chamber (15 mm × 9 mm) created by cut-outs in laminating adhesive on a substrate slide. The chamber was covered by a capping slide with openings on both ends.

Layer preparation

To determine the influence of several parameters on the release kinetics, we define "standard conditions" to prepare gelatin/antibody-conjugate layers and investigate variations thereof. Under "standard conditions", gelatin powder was dissolved in milliQ water at 37°C for 1 h while stirring. The solution was centrifuged at 21000×*g* for 10 min at 37°C and the supernatant was used for all further experiments. A casting solution containing 0.2%w/v gelatin and 1.5 µg/ml allophycocyanin conjugated antiCD3 IgG (IgG, clone SK7, ~260 kDa, BD) was prepared. 20 µl of this solution was cast onto the

flow chamber. The solution was dried at 20°C in ambient atmosphere with ~40% relative humidity (RH) to obtain a layer with a thickness of ~0.5 µm in the central region. By varying the volume of the same casting solution, we obtained layers of various thicknesses and determined the influence of the layer thickness on the release time. As a control, pure IgG solution without addition of gelatin was cast on a substrate slide. Since the pure IgG solution also contains trace amounts of gelatin as stabilizing agent, the thickness of this control layer is estimated to be 6 nm.

The effect of increased temperature (35°C and 40°C), increased humidity (85% RH) or reduced pressure (*in vacuo*) during the drying process on the release kinetics was determined.

Released molecules

The influence of the antibody size on the release kinetics, was studied by replacing IgG with a larger antibody, allophycocyanin conjugated IgM (IgM, ~1495 kDa, Ebioscience) and with smaller antibody fragments conjugated with smaller fluorophores: $F(ab')_2$-Alexa Fluor®647 (Fab, ~110 kDa, Cell Signaling) and Fc-Dylight®650 (Fc, ~50 kDa, Abcam).

Fluorescence imaging

A custom-built fluorescence imaging system was used to measure the release kinetics. Light from a red LED (625±10 nm, CBT-40, Luminus Devices), passing through a 650 nm short pass filter (Semrock), is used to excite the fluorophores in the sample. The emitted fluorescence passes through a 685/40 nm band pass filter (Semrock) and is imaged at 1.7× magnification by a CCD camera (SBIG). Details of the imaging setup have been described previously.[17]

Layer characterization

The topography of gelatin/antibody-conjugate layers was determined using a white light interferometer (smartWLI-microscope, GBS) with about 10 nm resolution. Scraping off a small area in the central region of the gelatin layer allowed us to use the substrate as a reference. Fig. 2a shows the thickness distribution of a representative gelatin/IgG layer with smooth surface. The similar pattern of antibody distribution (fluorescence readout) shown in Fig. 2b indicates no significant de-mixing of gelatin and IgG in the dry layer. To establish a correlation between thickness and fluorescence of gelatin/IgG layers, a region of interest (ROI) of 0.5 mm × 0.5 mm located adjacent to the scratch was defined. The average thickness and the fluorescence intensity of ROIs in layers prepared under different conditions were measured. As shown in Fig. 3, the average thickness of a ROI is proportional to its fluorescence intensity.

Measurement of equilibrium mass swelling ratios

To determine the equilibrium mass swelling ratios of gelatin layers prepared under different conditions, three Petri dishes (⌀: 3 cm) were filled with 5 ml of 0.2%w/v gelatin solution each and dried under different conditions: 40% RH 20°C, 40% RH 40°C and 85% RH 20°C. After drying, gelatin layers of ~10 mg

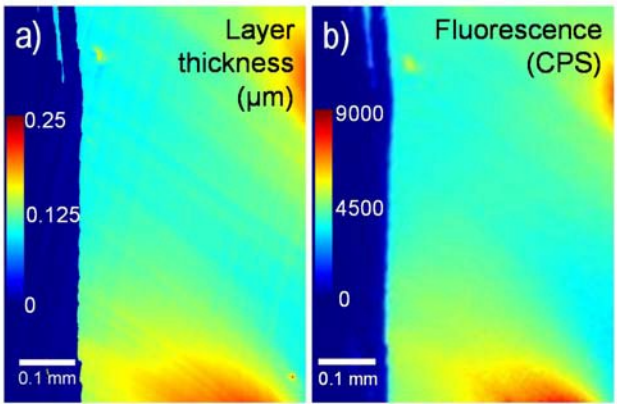

Fig. 2: The contour plot (a) and fluorescence image (b) of a dry gelatin/IgG layer.

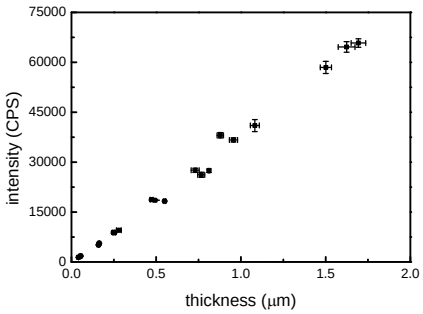

Fig. 3: Calibration of the fluorescence intensity of the layer against the layer thickness. Data points represent mean ± standard deviation (n=3).

were obtained. 5 ml of PBS was added to each Petri dish to incubate the layer at 20°C overnight. No further weight increase was found for longer incubation times. Excess water from the surface was removed by filter paper before the swollen layers were weighed. After that, the swollen layers were dried again, and their weights did not differ from the initial values, suggesting negligible dissolution and loss of gelatin during incubation and excess water removal. The equilibrium mass swelling ratio was calculated by dividing the weight of the swollen layer by the weight of the initial layer. As the swelling is a one dimensional expansion in the experiments, the thickness of the swollen layer can be calculated from the thickness of the dry layer and the equilibrium mass swelling ratio, when assuming the density of gelatin to be 1.3 g/cm^3. [20]

Measurement of release kinetics in flow chambers

Phosphate buffered saline (PBS) was used as the standard medium to flow at a rate of 1 µl/s through the chip. This flow rate was chosen to mimic the filling of the cell counting chambers by capillary action. In addition, we compared the release kinetics in the standard medium (PBS) with those in blood plasma and milliQ water. Fluorescence images of the cast layers were taken with 1 s exposure time at 5 s intervals. The excitation light was switched off between exposures to minimize bleaching. The fluorescence intensity of the layer was used to quantify the remaining IgG in the layer during the

release process. Regions of interest (ROIs) of the layer with a specific thickness were selected. The thickness was calculated from the fluorescence intensity of the ROI and verified by white light interferometry in several cases. The fluorescence intensities of each of these ROIs was analyzed for all successive images to study the release kinetics. The statistical analysis of different release kinetics is described in the ESI section "Statistical analysis of different release kinetics".

Measurement of antibody distribution and intensity of stained cells in counting chambers

Gelatin/IgG layers with two different thicknesses, 0.25 µm and 0.5 µm, were cast in cell counting chambers. A fluorescence image of each cell counting chamber (in the dry state) was recorded before 5 µl of blood was added to the filling port of the chamber and left to fill the chamber by capillary flow. Immediately after inflow a fluorescence image of the filled chamber was taken. The fluorescence intensity of a chamber without gelatin/IgG layer (autofluorescence of the chamber materials) was subtracted from the fluorescence images.

A normalized image was then obtained from the ratios of fluorescence intensities of the filled and unfilled chamber in the background-corrected images. This image is assumed to represent the ratio between antibody concentration after and before blood inflow. We also verified that the fluorescence intensity of APC does not change significantly between the wet and the dry state and that the absorption of (red) excitation and emission light by blood can be neglected. After 15 min incubation, another image was taken and image analysis software (ImageJ[21]) was used to identify ROIs (a few pixels), which were assigned to target cells, and quantify the integrated intensity within each ROI, i.e. of each identified cell (after background subtraction).

Results and discussion

Diffusion-controlled release mechanism and the influence of layer thickness on the release

Gelatin/IgG layers with thicknesses between 0.25 µm and 1.5 µm were prepared under "standard conditions" (see above), cast on flow chambers. The fluorescence intensities of these gelatin layers, corresponding to the amount of IgG in the layer, were monitored during the release process. Fig. 4a shows the fractional release of IgG from gelatin layers. The percentage (M_t/M_{total}) of released antibody as a function of time was calculated using the IgG, released from the layer at time t, (M_t) and the total (initial) IgG, embedded in the layer (M_{total}). Clearly, the release of IgG from gelatin layers is delayed when compared to the control without gelatin, and the thicker the gelatin layer the slower the release. The data plotted as a function of the square root of time in Fig. 4a demonstrates that

$$\frac{M_t}{M_{\text{total}}} = \left(\frac{t}{\tau}\right)^{1/2} \qquad (1)$$

during the initial phase of the release process[22], which allows us to extract release times from the shown fits. The $t^{1/2}$ dependence is characteristic of Fickian diffusion, suggesting the initial release is diffusion-controlled.[23] The release time τ from a thin slab of material in a diffusion-controlled system can be expressed as[24]:

$$\tau = \frac{\pi L^2}{4D} \qquad (2)$$

where D is the diffusivity of IgG in the gelatin layer, and L is the layer thickness. The measured release kinetics demonstrates that D/L^2 is constant during the initial phase of the release process, which can be interpreted as a constant diffusivity following a much faster swelling process. The resulting diffusivities assuming instantaneous swelling to the equilibrium mass swelling ratio of ~13.5 (Fig. 5), determined from the water uptake of bulk gelatin, corresponding to a height ratio of 17.2, are given in Table 1. As the diffusivity is independent of the thickness of the dry layer, the measured release time is proportional to the square of the dry layer thickness (Fig. 4b), which allows us to tune release kinetics by choosing an appropriate layer thickness. The diffusivity of IgG in a swollen gelatin layer is two orders of magnitude lower than that in PBS[25, 26], again, confirming that the release is delayed by embedding IgG in gelatin layers. Alternatively, instead of an instantaneous swelling followed by antibody release with a constant diffusivity, swelling and diffusion might also take place simultaneously with $D \propto L^2$, as expected (approximately) for a "jump diffusion"[27] mechanism. This case may require an alternative definition of the diffusivity, but would not affect the rest of the discussion.

Table 1: Release time (τ) and diffusivity ($D_{\text{swollen layer}}$) of IgG in swollen gelatin layers with varying thicknesses. All values represent mean ± standard deviation (n=3). As the 1.5 µm layers swell to almost the complete height of the chamber, the release from these layers was measured in both ~27 and ~52 µm high chambers and no significant differences were observed (see Fig. S2 in the ESI).

Thickness (µm) dry/swollen	τ (s)	$D_{\text{swollen layer}}$ (µm²/s)
0.25/4.3	23±4	0.63±0.10
0.50/8.6	88±12	0.65±0.08
0.75/12.9	176±34	0.74±0.11
1/17.2	392±30	0.59±0.03
1.5/25.8	647±27	0.79±0.04

Influence of layer preparation conditions on the release and possible mechanism

In diffusion-controlled release, the mobility of embedded molecules is dependent on the porosity of the hydrogel matrix.[28] It is described by the mesh size which is affected by the degree of (physical) crosslinking of hydrogels.[29] General physical crosslinking in hydrogels results from the random entanglement of disordered chains. In addition to these crosslinks, gelatin can take on a more ordered helical conformation involving three separate helical chains during the drying process[30], essentially increasing its degree of physical crosslinking. The formation of these triple helices and, thus, the degree of physical crosslinking of the gelatin layer can be influenced by the preparation conditions of gelatin layers. It has been reported that gelatin layers dried at 20°C or lower ("cold films") contain collagen-like triple helices, while layers dried above 35˚C ("hot films") are solely comprised of random coils.[31, 32] In the case of cold films, where triple helix formation is possible, higher humidity (contributing more water content in gelatin to stabilize helices via hydrogen bonds[30]) and longer drying times (allowing for the slow helix formation process[33]) promote helix formation.

The mass swelling ratio (between swollen and dry state) of hydrogels is known to strongly depend on the average distance between crosslinks (given as average mass of monomers between crosslinks), i.e. the mesh size.[29, 34] This makes the swelling ratio an excellent measure of the conformational state of gelatin with regard to its degree of crosslinking due to triple helix formation.[35] We therefore determined the mass swelling ratio of gelatin layers prepared under different conditions, for which different degrees of crosslinking were to be expected.

Fig. 5 shows that layers dried at lower temperature and higher RH show a smaller equilibrium mass swelling ratio, indicating smaller pore size and a larger degree of crosslinking, in agreement with expectations as well as previous findings.[30] This change of conformation with changing temperature and humidity was further corroborated by Fourier Transform Infrared (FT-IR) spectroscopy (see Fig. S5, Table S1 in the ESI).

In order to study the effect of this gelatin-intrinsic type of crosslinking on reagent release, we examined the release of antibody from cast gelatin layers dried under different conditions. And indeed, as shown in Fig. 6, layers dried at higher temperature show faster release, probably due to a lower degree of physical crosslinking as a consequence of reduced formation of triple helices in layers dried at higher temperatures.

Likewise in Fig. 7, layers dried in a humidity chamber (~85% RH), indeed show a slower release than layers dried under ambient atmosphere (~40% RH), confirming that the formation of triple helices is very likely to play a role in the fine-tuning of release characteristics of gelatin layers. In addition, it is noticeable in Fig. 7, that the release from layers dried *in vacuo* is much faster than the release from layers prepared under ambient pressure. This may be ascribed to a lower degree of

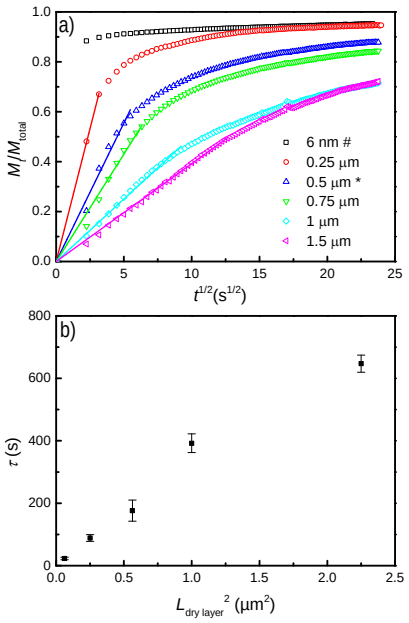

Fig. 4: (a) Representative release curves (symbols) of IgG from layers of varying thicknesses and their corresponding fits to $M_t/M_{total}=(t/\tau)^{1/2}$ (lines). The asterisk indicates "standard conditions" and the hash indicates the control without (additional) gelatin. (b) Release time (τ) obtained from three independent release experiments as a function of the square of the thickness of the dry layer. Data points represent mean ± standard deviation (n=3).

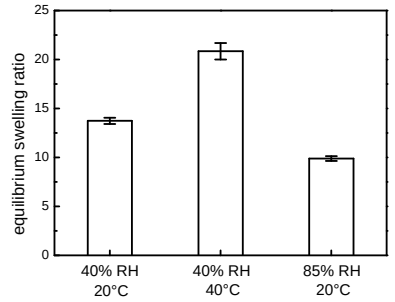

Fig. 5: Equilibrium mass swelling ratios of gelatin layers prepared under different temperatures and humidities. Data represents mean ± standard deviation (n=4).

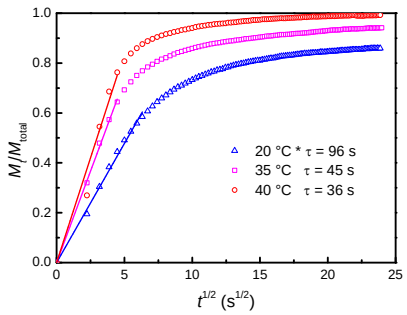

Fig. 6: Representative release curves (symbols) of IgG from 0.5 µm thick gelatin layers dried at different temperatures and fits of the initial release according to Eq. (1) (lines). The asterisk indicates "standard conditions". Release times (τ) are values for the specific release experiments shown here.

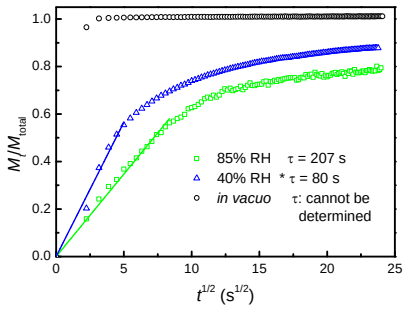

Fig. 7: Representative release curves(symbols) of IgG from 0.5 µm thick layers dried under reduced pressure (0.2 bar, black circles), ambient atmosphere (blue triangles) and 85% RH (green squares) and fits of the initial release according to Eq. (1) (lines). The asterisk indicates "standard conditions". Release times (τ) are values for the specific release experiments shown here.

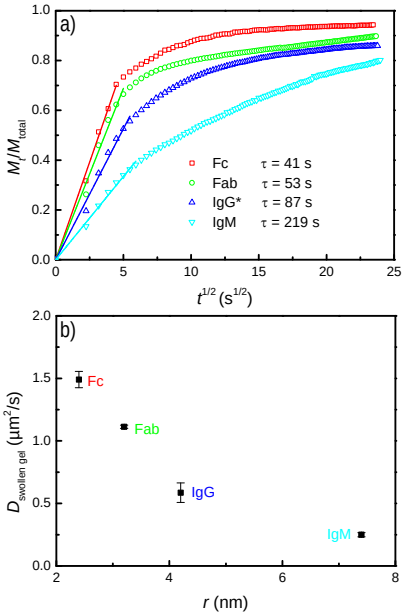

Fig. 8: (a) Representative release curves (symbols) of antibodies with different MWs from 0.5 µm thick layers and fits of their initial release according to Eq. (1) (lines). The asterisk indicates "standard conditions". Release times (τ) are values for the specific release experiments shown here. (b) Diffusivity ($D_{swollen\ layer}$) of antibodies and antibody fragments. Data points represent mean ± standard deviation (n=3).

physical crosslinking of gelatin due to faster drying and lower water content compared to the ambient atmosphere. The formation of triple helices in gelatin is believed to be a process taking place on a timescale of many hours.[33] Therefore it is not surprising that drying *in vacuo*, taking about 5 min, is too short to allow for considerable formation of triple helices. In contrast, ambient (~40% RH) and humid (~85% RH) atmosphere maintain sufficient moisture content in the gelatin and extend the drying period to approximate 30 min and 2 days, respectively, thus facilitating extensive formation of triple helices.

Table 2 summarizes the release times in gelatin layers prepared under different conditions.

In conclusion, low temperature, high humidity and long drying period, result in slower release and are probably due to the formation of a larger amount of triple helices, increasing the degree of physical crosslinking and thus decreasing the mesh size.

Influence of reagent size on the release

In addition to the structure of the release layer, the size of released reagent also has an impact on diffusion-controlled release.[36-40] Four types of antibody and antibody fragments with different molecular weights (MWs) were chosen to study the influence of the reagent size on the release. The radii of the antibodies were calculated using

$$r[\mathrm{nm}] = 0.066 \times (MW[\mathrm{Da}])^{1/3} \qquad (3)$$

which assumes the antibody to be spherical, having a density of 1.38 g/cm^3.[41] Gelatin layers were prepared under "standard conditions". Fig. 8a clearly shows that the larger the protein the slower the diffusion. The $t^{1/2}$ dependence in the initial phase of the release process points at a Fickian diffusion-controlled release behavior. Fig. 8b shows that there is an inverse correlation between diffusivity and molecular radius. The observed influence of molecular size on the diffusivity is in agreement with the findings obtained from other collagen[42, 43] and gelatin[44] based release systems.

Influence of electrostatic interactions on the release

Electrostatic interactions between gelatin and any embedded antibody influence the release kinetics of antibodies from the gelatin matrix and can be influenced by the physicochemical properties of the release medium.[45] Therefore, blood plasma, PBS and milliQ water were compared as release media to study the influence of the medium on the release of IgG from gelatin layers. As shown in Fig. 9, the release times of IgG in PBS (82±15 s, n=3) and blood plasma (82±10 s, n=3) are similar to each other and much shorter than in milliQ water. Additionally, considerably more IgG seems to stay trapped in the layer in milliQ water compared to PBS and plasma. Since both gelatin and IgG contain charged functional groups, the ions in PBS are presumed to screen surface charges, reducing the interaction between gelatin and antibodies, thereby favoring the detachment of antibody from the gelatin matrix. In milliQ water, such screening is much reduced, which should result in longer release times (312±51 s, n=3) and less antibody release, which is indeed the case. The finding that antibody release in

Table 2: Release times (τ) of IgG in swollen gelatin layers with initial thickness of 0.5 µm dried under different conditions. All values represent mean ± standard deviation (n=3).

T(°C)	atmosphere	τ (s)
20	85% RH	194±14
20	40% RH	88±12
35	40% RH	46±4
40	40% RH	35±1
20	*in vacuo*	N.A.

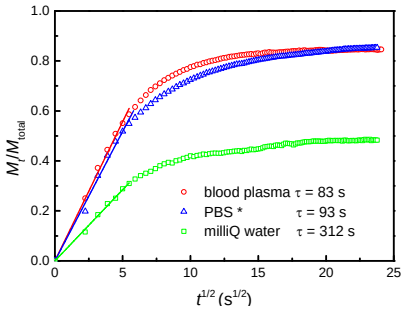

Fig. 9: Representative release curves (symbols) of IgG from 0.5 µm thick layers in blood plasma (red squares), PBS (blue triangles) and milliQ water (green squares) and fits of their initial release according to Eq. (1) (lines). The asterisk indicates "standard conditions". Release times (τ) are values for the specific release experiments shown here.

blood plasma and PBS are comparable supports this explanation, as the ion concentration in blood plasma is similar to that in PBS.

These results also prove that PBS is a suitable medium to replace blood plasma in release studies.

Implication of antibody release kinetics for on-chip cell staining.

Finally, we proceeded to verify that the expected release kinetics has an immediate effect on the antibody distribution in the final application, a cell counting chamber after blood inflow, and consequently can help to improve the quality of cell staining. We compared a cell counting chamber containing a 0.25 µm thick gelatin layer with an expected fast release (τ=20 s) with one containing a 0.5 µm thick layer with an expected slow release (τ=88 s). The measured ratios between antibody concentrations after and before blood inflow, plotted against the distance from the filling port, are shown in Fig. 10a. Clearly, the 0.5 µm thick layer shows a much flatter intensity profile than the 0.25 µm layer, i.e. the 0.5 µm thick layer prevents wash-off during blood inflow, which takes about 5-10 s, much better than the 0.25 µm thick layer. In the case of fast release from a 0.25 µm thick layer, the inflowing blood washes off about 70% of the antibody close to the filling port and transports it towards the venting port, where the antibody concentration roughly doubles. In contrast, the antibody in a chamber with a 0.5 µm thick layer changes by less than 20% throughout the whole length of the chamber. To illustrate that the improvement in antibody distribution directly translates into improved cell staining, we determine the fluorescence intensities of T-lymphocytes ($CD3^+$) after 15 min incubation in the "filling region" (0-1 mm from the filling port) and the "venting region" (0-1 mm from the venting port) and translate this intensity to the number of IgGs bound per cell by means of the calibration which is described in the ESI section "Quantification of embedded IgG in gelatin layers". Histograms of the number of antibody molecules bound per cell in these regions are shown in Fig. 10b. The increased antibody concentration close to the venting port in the chamber with the 0.25 µm layer does not result in significantly increased fluorescence intensity per cell (saturation) and it only reduces the signal-to-background ratio, as the simple design of the cell counting chambers does not allow for a washing step. In contrast, the reduced concentration close to the filling port results in significantly reduced cell intensities. As a consequence of the relatively homogeneously distributed antibody in the chamber with the 0.5 µm thick layer, cell intensities are homogeneous throughout the full length of the chamber. The obtained saturation intensity matches well with the reported CD3 antibody binding capacities on T-cells between 60k and 70k[46]. Using the calibration of fluorescence intensity against antibody concentration (see Fig. S4 in the ESI), we can quantitatively monitor the progress of antibody binding in real time. Quantitative information on the saturation is of great use to assess and later fine-tune assay parameters, such as antibody concentration, incubation time or minimum needed and maximum attainable cell intensities.

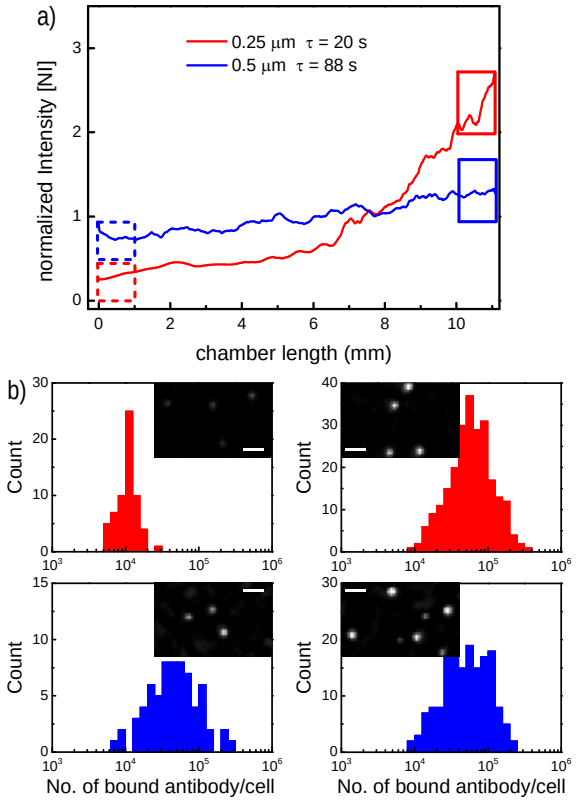

Fig. 10: (a) IgG distribution in cell counting chambers with a 0.25 µm (red) and a 0.5 µm thick (blue) layer after blood inflow. Dashed squares and solid rectangles denote the "filling region" and "venting region", respectively. (b) Histograms of the amount of bound antibodies per cell at the "filling region" (left panel) and "venting region" (right panel) in the chambers with 0.25 µm (red) and 0.5 µm (blue) thick gelatin layers after 15 min incubation. The insets are zoom-in fluorescence images of stained cells from a representative area in the "filling and venting regions". The white dots are identified cells. Intensity scale: 0 (black) to 2000 camera units per second/CPS (white). Scale bars: 50 µm.

To briefly summarize, we have shown the close correlation between the antibody release time, the resulting antibody distribution across our cell counting chambers and thus, the homogeneity of cell staining. By choosing preparation conditions judiciously, based on this study, optimal cell staining for our cell counting application can be achieved.

Conclusions

We have studied the release kinetics of antibodies embedded in gelatin layers with (sub-) µm-scale thicknesses on second to minute timescales. The gelatin layers were monitored by real-time and *in situ* fluorescence imaging during the release in a flow chamber. Under most conditions, the initial phase of antibody release from cast layers is proportional to $t^{1/2}$, indicating diffusion-controlled release. The quadratic dependence of the release time on the thickness of the dry layer confirms this mechanism. The release is strongly influenced by the size of the antibody or antibody fragment in the gelatin layer and by the ion content of the medium. By varying the temperature, humidity and drying time during the preparation of gelatin matrices for reagent release, we can influence the material properties of the layer and thereby control reagent release times. In the final application, a cell counting chamber, the release time is shown to determine the antibody distribution throughout the chamber, which in turn governs the spatial distribution of cell staining intensities. This proves that the knowledge of the release kinetics in flow chambers, can be translated into the performance of reagent-sample mixing in cell counting chambers. The insights gained here, on how to tune release times of antibodies from gelatin layers enable us to tailor on-chip sample preparation in cell counting chambers. Moreover, the concept of this study can be extended to investigate on-chip release of a variety of reagents (i.e. lysis agents, fluorescent dyes, enzymes and drugs) from a hydrogel matrix. The understanding of the release kinetics of these reagents can be translated to tune the sample-reagent mixing in a multitude of microfluidic devices and optimize on-chip sample preparation for many biological assays.

Acknowledgements

This work was funded by the European Research Council under grant number 282276.

References

1. W. Weaver, H. Kittur, M. Dhar and D. Di Carlo, Lab Chip, 2014, 14, 1962-1965.
2. C. D. Chin, V. Linder and S. K. Sia, Lab Chip, 2012, 12, 2118-2134.
3. V. Gubala, L. F. Harris, A. J. Ricco, M. X. Tan and D. E. Williams, Anal Chem, 2012, 84, 487-515.
4. L. Gervais, N. de Rooij and E. Delamarche, Advanced Materials, 2011, 23, H151-H176.
5. M. Hitzbleck and E. Delamarche, Chemical Society Reviews, 2013, 42, 8494-8516.
6. B. Weigl, G. Domingo, P. LaBarre and J. Gerlach, Lab Chip, 2008, 8, 1999-2014.
7. T. van Oordt, Y. Barb, J. Smetana, R. Zengerle and F. von Stetten, Lab Chip, 2013, 13, 2888-2892.
8. D. Czurratis, Y. Beyl, A. Grimm, T. Brettschneider, S. Zinober, F. Larmer and R. Zengerle, Lab Chip, 2015, 15, 2887-2895.
9. R. Boden, M. Lehto, J. Margell, K. Hjort and J. A. Schweitz, J Micromech Microeng, 2008, 18.
10. J. Hoffmann, D. Mark, S. Lutz, R. Zengerle and F. von Stetten, Lab Chip, 2010, 10, 1480-1484.
11. D. Y. Stevens, C. R. Petri, J. L. Osborn, P. Spicar-Mihalic, K. G. McKenzie and P. Yager, Lab Chip, 2008, 8, 2038-2045.
12. E. Fu, B. Lutz, P. Kauffman and P. Yager, Lab Chip, 2010, 10, 918-920.
13. M. Hitzbleck, L. Gervais and E. Delamarche, Lab Chip, 2011, 11, 2680-2685.
14. S. Q. Jin, M. H. Dai, B. C. Ye and S. R. Nugen, Microsyst Technol, 2013, 19, 2011-2015.
15. L. Gervais and E. Delamarche, Lab Chip, 2009, 9, 3330-3337.
16. J. Kim, D. Byun, M. G. Mauk and H. H. Bau, Lab Chip, 2009, 9, 606-612.
17. M. Beck, S. Brockhuis, N. van der Velde, C. Breukers, J. Greve and L. W. M. M. Terstappen, Lab Chip, 2012, 12, 167-173.
18. M. Mortato, L. Blasi, G. Barbarella, S. Argentiere and G. Gigli, Biomicrofluidics, 2012, 6, 44107.
19. A. N. Zelikin, Acs Nano, 2010, 4, 2494-2509.
20. GMIA, Gelatin Handbook, Gelatin Manufacturers Institute of America, New York, 2012.
21. C. A. Schneider, W. S. Rasband and K. W. Eliceiri, Nature Methods, 2012, 9, 671-675.
22. T. Higuchi, J Pharm Sci, 1961, 50, 874-875.
23. H. L. Frisch, Polym Eng Sci, 1980, 20, 2-13.
24. J. Siepmann, R. Siegel, A. and M. Rathbone, J., Fundamentals and Applications of Controlled Release Drug Delivery, Springer, New York, 1st edn., 2012.
25. M. L. Radomsky, K. J. Whaley, R. A. Cone and W. M. Saltzman, Biomaterials, 1990, 11, 619-624.
26. E. A. Schnell, L. Eikenes, I. Tufto, A. Erikson, A. Juthajan, M. Lindgren and C. de Lange Davies, J Biomed Opt, 2008, 13, 064037.
27. N. A. Peppas and C. T. Reinhart, Journal of Membrane Science, 1983, 15, 275-287.
28. Y. Wu, S. Joseph and N. R. Aluru, J Phys Chem B, 2009, 113, 3512-3520.
29. C. C. Lin and A. T. Metters, Adv Drug Deliver Rev, 2006, 58, 1379-1408.
30. P. V. Kozlov and G. I. Burdygina, Polymer, 1983, 24, 651-666.
31. E. Bradbury and C. Martin, P Roy Soc Lond A Mat, 1952, 214, 183-192.
32. M. Djabourov and P. Papon, Polymer, 1983, 24, 537-542.
33. S. B. Rossmurphy, Polymer, 1992, 33, 2622-2627.
34. M. N. Mason, A. T. Metters, C. N. Bowman and K. S. Anseth, Macromolecules, 2001, 34, 4630-4635.
35. A. Bigi, S. Panzavolta and K. Rubini, Biomaterials, 2004, 25, 5675-5680.

36. M. Henke, F. Brandl, A. M. Goepferich and J. K. Tessmar, Eur J Pharm Biopharm, 2010, 74, 184-192.
37. N. K. Reitan, A. Juthajan, T. Lindmo and C. de Lange Davies, J Biomed Opt, 2008, 13, 054040.
38. F. Brandl, F. Kastner, R. M. Gschwind, T. Blunk, J. Tessmar and A. Gopferich, J Control Release, 2010, 142, 221-228.
39. N. Fatin-Rouge, K. Starchev and J. Buffle, Biophys J, 2004, 86, 2710-2719.
40. A. A. Dinerman, J. Cappello, H. Ghandehari and S. W. Hoag, J Control Release, 2002, 82, 277-287.
41. H. P. Erickson, Biological Procedures Online, 2009, 11, 32-51.
42. T. Kihara, J. Ito and J. Miyake, PLoS One, 2013, 8, e82382.
43. D. L. Gilbert, T. Okano, T. Miyata and S. W. Kim, Int J Pharm, 1988, 47, 79-88.
44. Y. E. Fang, Q. Cheng and X. B. Lu, Journal of Applied Polymer Science, 1998, 68, 1751-1758.
45. Y. Tabata and Y. Ikada, Adv Drug Deliver Rev, 1998, 31, 287-301.
46. L. Ginaldi, M. De Martinis, A. D'Ostilio, L. Marini, F. Loreto, M. Modesti and D. Quaglino, Am J Hematol, 2001, 67, 63-72.